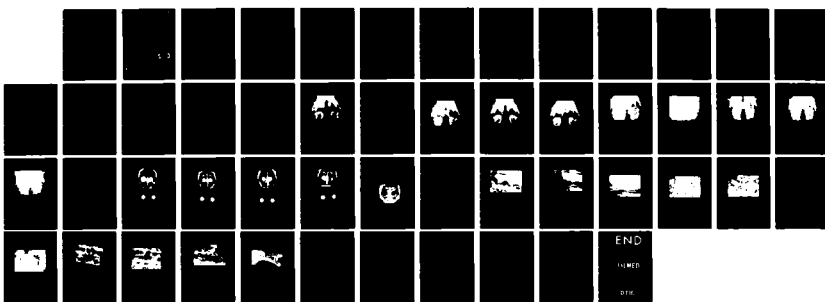
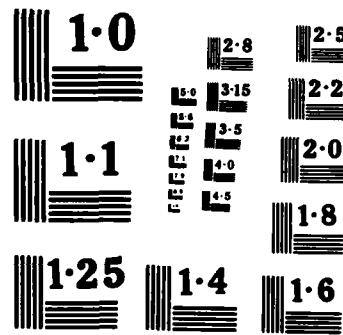


AD-A157 996 MANAGEMENT OF HARD TISSUE AVULSIVE WOUNDS AND 1/1
MANAGEMENT OF OROFACIAL FRACTURES(U) BATTELLE COLUMBUS
LABS OH C R HASSSLER ET AL. 19 MAY 83 DAMD17-82-C-2168
UNCLASSIFIED F/G 6/5 NL





NATIONAL BUREAU OF STANDARDS
MICROCOPY RESOLUTION TEST CHART

AD-A157 996

AD

2

ANNUAL REPORT

Contract No. DAAB17-82-C-2168

ON

MANAGEMENT OF HARD TISSUE AVULSIVE WOUNDS
AND MANAGEMENT OF OROFACIAL FRACTURES

to

U.S. ARMY MEDICAL RESEARCH
AND DEVELOPMENT COMMAND
Fort Detrick,
Frederick, Maryland 21701-5012

May 19, 1983

by

Craig R. Hassler and Larry G. McCoy

BATTELLE
Columbus Laboratories
505 King Avenue
Columbus, Ohio 43201

DOI DISTRIBUTION STATEMENT

DTIC FILE COPY

DTIC
ELECTED
AUG 15 1985
S D
B

Approved for public release; distribution unlimited.

The findings in this report are not to be
construed as an official Department of the Army position
unless so designated by other authorized documents.

85 89 085

The overall objective is to produce a completely resorbable biomaterial which will promote bone formation and via a bone remodeling--biodegradation process be completely replaced by bone. It should be pointed out that the dynamics of this situation are complex. The biomaterial should allow bone ingrowth and provide mechanical integrity during the remodeling, biodegradation process. The dissolution of the biomaterial and bone formation need to proceed in a parallel and controlled fashion, so that mechanical integrity of the area under repair is not lost. In early studies, omnidirectional structural material would, depending upon chemical composition, either: not entirely biodegrade, or would degrade until mechanical integrity was lost. Unidirectional materials, as reported previously in our Annual Reports for Contract No. DADA17-69-0-9118 (dated May 31, 1981 and May 31, 1982) were free of these problems; ingrowth and subsequent bioresorption without loss of implant integrity was noted.

"First Generation" Unidirectional Material utilized to prove the concept, had low pore density and poor mechanical strength. The materials utilized the present in vivo investigation were calendered or rolled to form a serrated surface and then stacked and sintered together to form a unique unidirectional porosity as required by the particular implant situation. We have termed this the "second generation" Material. The technique allows directional porosity material to be formed in blocks of high-strength material with continuous pores of large diameter. The pores can be specifically oriented, and the surrounding material can be made dense enough to provide a high-strength scaffold.

Implants 8 mm in diameter were placed bilaterally in the calvaria of the animals and were evaluated for periods of 3, 6, 9, and 12 months. At each time period, a portion of the animal population was necropsied and analyzed by histologic and radiographic methods. The results of the in vivo study indicate that unidirectional porosity will allow bone ingrowth and biodegradation without loss of implant integrity. These results are in agreement with our previous in vivo unidirectional material experiments. The analysis suggests that the concept of large diameter porosities, oriented in the direction of desired bone growth, is feasible. This study demonstrates a practical method of producing the desired material with adequate pore density.

The above mentioned materials "second generation" were utilized in the animal experiments included in this report. The present ceramics development effort produced even higher quality and strength materials which we have termed the "third generation materials". This third generation material has the identical chemical formulation as the second generation material. However, a hot extrusion technique was employed. This produces a stronger block material with minimal delamination problems. Further improvement of third generation material is now in progress.

SUMMARY

Research studies were conducted to produce and evaluate a high-quality directional porosity resorbable calcium phosphate ceramic material for use in the management of hard tissue avulsive wounds and orofacial fractures. The previous efforts demonstrated that directional porosity would allow adequate ingrowth of bone through the biomaterial prior to loss of mechanical integrity of the biomaterial.

The overall objective is to produce a completely resorbable biomaterial which will promote bone formation and via a bone remodeling--biodegradation process be completely replaced by bone. It should be pointed out that the dynamics of this situation are complex. The biomaterial should allow bone ingrowth and provide mechanical integrity during the remodeling, biodegradation process. The dissolution of the biomaterial and bone formation need to proceed in a parallel and controlled fashion, so that mechanical integrity of the area under repair is not lost. In early studies, omnidirectional structural material would, depending upon chemical composition, either: not entirely biodegrade, or would degrade until mechanical integrity was lost. Unidirectional materials, as reported previously in our Annual Reports for Contract No. DADA17-69-0-9118 (dated May 31, 1981 and May 31, 1982) were free of these problems; ingrowth and subsequent bioresorption without loss of implant integrity was noted.

"First Generation" Unidirectional Material utilized to prove the concept, had low pore density and poor mechanical strength. The materials utilized the present in vivo investigation were calendered or rolled to form a serrated surface and then stacked and sintered together to form a unique unidirectional porosity as required by the particular implant situation. We have termed this the "second generation" Material. The technique allows directional porosity material to be formed in blocks of high-strength material with continuous pores of large diameter. The pores can be specifically oriented, and the surrounding material can be made dense enough to provide a high-strength scaffold.

Implants 8 mm in diameter were placed bilaterally in the calvaria of the animals and were evaluated for periods of 3, 6, 9, and 12 months. At each time period, a portion of the animal population was necropsied and analyzed by histologic and radiographic methods. The results of the in vivo study indicate that unidirectional porosity will allow bone ingrowth and biodegradation without loss of implant integrity. These results are in agreement with our previous in vivo unidirectional material experiments. The analysis suggests that the concept of large diameter porosities, oriented in the direction of desired bone growth, is feasible. This study demonstrates a practical method of producing the desired material with adequate pore density.

The above mentioned materials "second generation" were utilized in the animal experiments included in this report. The present ceramics development effort produced even higher quality and strength materials which we have termed the "third generation materials". This third generation material has the identical chemical formulation as the second generation material. However, a hot extrusion technique was employed. This produces a stronger block material with minimal delamination problems. Further improvement of third generation material is now in progress.

DTIC
ELECTE
S AUG 15 1985 D

B

ii



A-1

Accession For	
NTIS	7481
Pub. Ed.	<input checked="" type="checkbox"/>
Unpublished	<input type="checkbox"/>
Spec. Edition	<input type="checkbox"/>
By	
Distribution	
Availability Codes	
Dist	Avail and/or Special

FOREWORD

In conducting the research described in this report, the investigator adhered to the "Guide for the Care and Use of Laboratory Animals", prepared by the Committee on Care and Use of Laboratory Animals of the Institute of Laboratory Animal Resources, National Research Council (DHEW Publication No. (NIH) 78-23, Revised 1978).

TABLE OF CONTENTS

	<u>Page</u>
BACKGROUND, PROBLEM AND APPROACH	1
MATERIALS AND METHODS	3
Task 1. Prepare Tricalcium Phosphate Powder	3
Task 2. Characterize the Tricalcium Phosphate Powder for Chemical Composition and Physical Properties	3
Task 3. Conduct Study on Ceramic-Organic Mix Formulation for Hot Extrusion Forming	4
Task 4. Produce Fluted Sheets to Form Tricalcium Phosphate Continuous Porosity Structures	5
Task 5. Build the Matrix Structure	6
Task 6. Cure and Remove the Organic Binders from the Matrix	6
Task 7. Sinter the Matrix Structure	6
Task 8. Preparation of Experimental Samples	7
Task 9. Characterization of the Matrix Structure	7
EXPERIMENTAL ANIMAL STUDIES	7
Research Protocol	7
Radiographic Examination of Tricalcium Phosphate Biodegradability	8
Histologic Evaluations	25
CONCLUSIONS AND DISCUSSION	37
RECOMMENDATIONS	39
REFERENCES	40

LIST OF FIGURES

Figure 1. Radiograph of Rabbit D-81, 21 Days Post-Implant	9
Figure 2. Radiograph of Rabbit D-81, 3 Months Post-Implant	11
Figure 3. Radiograph of Rabbit D-81, 6 Months Post-Implant	12
Figure 4. Radiograph of Rabbit D-81, 9 Months Post-Implant	13
Figure 5. Radiograph of Rabbit F-81, Immediately Post-Implant	14

LIST OF FIGURES
(Continued)

	<u>Page</u>
Figure 6. Radiograph of Rabbit F-81, 12 Months Post-Implant	15
Figure 7. Radiograph of Rabbit I-81, 3 Months Post-Implant	16
Figure 8. Radiograph of Rabbit I-81, 12 Months Post-Implant	17
Figure 9. Radiograph of Rabbit I-81, 9 Months Post-Implant	18
Figure 10. Three-Month Post-Necropsy Radiograph of Excised Calvarium from Rabbit G-81	20
Figure 11. Six-Month Post-Necropsy Radiograph of Excised Calvarium from Rabbit E-81	21
Figure 12. Nine-Month Post-Necropsy Radiograph of Excised Calvarium from Rabbit D-81	22
Figure 13. Twelve-Month Post-Necropsy Radiograph of Excised Calvarium from Rabbit F-81	23
Figure 14. Twelve-Month Post-Necropsy Radiograph of Excised Calvarium from Rabbit N-81	24
Figure 15. Photomicrograph of Tricalcium Phosphate Specimen with Directed Porosity, Three Months Post-Implant (Rabbit G-81-3L)	26
Figure 16. Photomicrograph of Tricalcium Phosphate Specimen with Directed Porosity, Three Months Post-Implant (Rabbit B-81-5T)	27
Figure 17. Photomicrograph of Bone Ingrowth Into Longitudinal Pore at High Magnification, Three Months Post-Implant (Rabbit B-81-5T)	28
Figure 18. Photomicrograph of Bone Ingrowth Into Tricalcium Phosphate, Six Months Post-Implant (Rabbit A-81-5L)	29
Figure 19. Photomicrograph of Bone Ingrowth Into Tricalcium Phosphate, Six Months Post-Implant (Rabbit A-81-5T)	30
Figure 20. Photomicrograph of Tricalcium Phosphate Six Months Post-Implant (Rabbit E-81-4T)	32

LIST OF FIGURES
(Continued)

	<u>Page</u>
Figure 21. Photomicrograph of Bone Ingrowth into Tricalcium Phosphate, Nine Months Post-Implant (Rabbit C-81-LFC)	33
Figure 22. Photomicrograph of Bone Ingrowth into Tricalcium Phosphate, Twelve Months Post-Implant (Rabbit F-81-L2)	34
Figure 23. Photomicrograph of Bone Ingrowth into Tricalcium Phosphate, Twelve Months Post-Implant (Rabbit T-81-L2)	35
Figure 24. Photomicrograph of Bone Ingrowth Into a Control Animal Twelve Months Post-Surgery (Rabbit N-81-5L)	36

LIST OF TABLES

Table 1. Powder Characterization	4
----------------------------------------	---

BACKGROUND, PROBLEM AND APPROACH

Historically, various techniques have been employed for the repair or treatment of osseous diseases, defects, and wounds. Autogeneous bone grafting remains the most satisfactory approach, but is not without the disadvantages associated with double surgeries, limits in structural properties, and the limitations imposed on the repair of massive osseous defects.

Since April, 1969, Battelle's Columbus Laboratories has been conducting research under contract to the U.S. Army Institute of Dental Research (USAIDR), to develop resorbable ceramics for potential application in the repair of hard tissue avulsive wounds. The basic materials have been calcium phosphates. These materials were selected because they contain two of the essential elements of the natural bone mineral phase, calcium hydroxyapatite.

In vivo studies were conducted initially at USAIDR, using the sintered porous materials and slurries prepared at Battelle from tricalcium phosphate $\text{Ca}_3(\text{PO}_4)_2$ and other calcium orthophosphate powders CaHPO_4 and $\text{Ca}(\text{H}_2\text{PO}_4)_2$, to evaluate the potential use of calcium phosphates to both facilitate repair of bone defects and to determine the best material for future exploration(1-3). The implant studies indicated that calcium phosphates consisting essentially of the mineral phases $\text{Ca}(\text{PO}_3)_2$, $\text{Ca}_3(\text{PO}_4)_2$, and CaHPO_4 are well tolerated by the tissue, appeared to be nontoxic, resorbable, and permitted rapid invasion of new bone.

Of the various porous calcium phosphate materials investigated, tricalcium phosphate, $\text{Ca}_3(\text{PO}_4)_2$, was selected for continued development and evaluation since it was easy to fabricate and was found to be both biocompatible and resorbable. Emphasis has been directed toward producing porous materials consisting of single-phase tricalcium phosphate(4-7). Research on granular formations of tricalcium phosphates (TCP) continued at USAIDR. Basic research at Battelle-Columbus was focused on producing practical large segment replacement implants from TCP.

To provide basic resorption rate data on the in vivo behavior of solid tricalcium phosphate bioresorbable ceramics, implant studies were initiated in 1975 at Battelle-Columbus using the rabbit calvarium model(8). Early samples of tricalcium phosphate were implanted as a control and samples

of two new materials were implanted for comparative observation. These new materials were prepared using improved processing techniques derived in previous materials development studies and represented significant improvements in the structural characteristics of porous tricalcium phosphate. The characterization of the materials involved and the results of the in vivo studies were the subject of the Fifth Report(8).

These results indicated that the improved material exhibited significant increases in resorption rate. In fact, the material resorbed so rapidly that after the ninth month the implant appeared to be granulated and was invaded with connective tissue. This result does not imply lack of biocompatibility, but does suggest that such rapid degradation can be deleterious in stress-bearing situations.

To determine the effects of structural variations on resorption rate, experimental porous implants were prepared using a single tricalcium phosphate powder with different pore size distribution. Three materials were prepared for in vivo evaluation. These studies demonstrated that orientation of pore structure is a more important variable than pore size distribution(9). The study indicated that a higher density material of the stoichiometric chemistry with directional porosity is probably the desired material.

The seventh report(10) demonstrated that the concept of directional porosity could provide a satisfactory result; adequate ingrowth of bone to provide mechanical integrity prior to loss of mechanical integrity of the tricalcium phosphate. These results were corroborated by Tortorelli(11). The material used in these experiments was far from ideal; consequently, a better method of production was sought. The eighth report outlines the development of a better material, the second generation material, and early phases of its in vivo evaluation(12). The ideal material should minimally inhibit the ingrowth of bone; consequently, large pores and a high pore density are desirable. The ideal material should also be of high strength and should have mechanical properties approaching bone. Consequently, a material of high density in the non-porous regions was sought. It was also deemed desirable to have a material that could be readily manufactured with the pore alignment and size required for a particular application.

The present report outlines the development of a higher quality "third generation" material which more closely approaches properties required for an ideal material. This report also contains the in vivo, results completed on "second generation" material. (This material is chemically identical to the third generation material now being produced, but it has lower mechanical strength.)

MATERIALS AND METHODS

The major material developments effort this year was the development of a third generation directional porosity material with improved mechanical properties. Several methods for the material were proposed. However, the hot extrusion forming was the method selected for extensive development and evaluation. The ceramic preparation was performed in a series of tasks. The tasks and their results are discussed in the following sections.

Task 1. Prepare Tricalcium Phosphate Powder

Calcium carbonate was combined with phosphoric acid to form a powder precipitate by slowly mixing these two components at 180°F. Once dried in air, the powders were dried under vacuum, 220°F, overnight. Approximately 6.4 kg of material in eight batches were prepared in this manner.

Task 2. Characterize the Tricalcium Phosphate Powder for Chemical Composition and Physical Properties

X-ray diffraction analysis of the above powder revealed it to be hydroxylapatite with a trace of monolite. The powder surface area was 13.6 m²/gm, which would indicate a mean particle size in the submicron range. To crush the large, hard agglomerates, formed during drying, the precipitate powder was dry ball milled for 2 hours in a polyethylene container with aluminum oxide balls. To convert the hydroxylapatite to whitlockite, the powder was calcined for 3-1/2 hours at 1500°F followed by an x-ray diffraction analysis. The powder was 100 percent converted to whitlockite. To break up

sintered agglomerates, the calcined powder was ball milled with hexane for 12 hours in a polyethylene jar with aluminum oxide balls. The following characterization was performed on the powder.

TABLE 1. POWDER CHARACTERIZATION

	As Produced	Ball Milled 2 Hours	Calcined at 1550°F HexaneBall Milled
Bulk density percent theoretical	10.3	17.4	23.1
Tap density percent theoretical	15.0	27.8	36.8
Surface area m^2/gm	13.57	16.4	TBD

Since the characteristics of this powder are similar to those of the powder produced in 1981, a sintering study of this powder was not undertaken. Within its usual sintering range, tricalcium phosphate has a destructive transformation from β to α form with the alpha form having a lower density. This conversion begins approximately at 2050°F and limits the sintering temperature of the tricalcium phosphate matrix to 2000°F.

Task 3. Conduct Study on Ceramic-Organic
Mix Formulation for Hot Extrusion Forming

When formulating mixes for hot extrusion or injection molding, one attempts to obtain the optimum binder content for molding. This optimum is a condition that represents a balance between maintaining the rheological condition for molding and a minimum amount of binder.

A practical method has been found for determining an optimum binder concentration for a given powder without making an elaborate characterization of the powder. The method is a modification of the ASTM D-281-31 oil adsorption test. The modification consists of the use of the Brabender Plastograph to minimize the operator variance factor.

In this method, the powder is mixed with an oil, the oil being added at a constant rate while the torque is recorded by the plastograph. The point at which the maximum torque occurs is interpreted as being the critical powder volume concentration (CPVC).

Expressed as an equation, CPVC becomes:

$$CPVC = \frac{\text{Volume of Powder}}{(\text{Volume of Powder} + \text{Volume of Oil})}$$

For tricalcium phosphate, the CPVC equalled 64.0 percent. Converting from a volume percentage to a weight percent, this optimum binder concentration is 14 weight percent organic and 86 weight percent tricalcium phosphate. From this, a ceramic-organic mix was formulated containing a plasticizer, a wax, and a surfactant, having a combined weight of 14 percent of the batch.

The tape casting process, used in 1981, contained 20.7 weight percent organic binder. This 6.7 weight percent reduction organic content, along with an improved forming technique, has resulted in improved sintered densities.

Task 4. Produce Fluted Sheets to Form Tricalcium Phosphate Continuous Porosity Structures

To obtain sheets of correct thickness, a die was purchased from Brabender Plastograph Company having the capability of extruding sheets ranging in thickness from 1.5 to 3.0 mm with a predetermined width of 25 mm. Using the mix formulated in Task 3, flat sheets 25 mm wide and 1.5 mm thick were formed by hot extrusion. An embossing tool was machined from a Teflon rod with circular grooves of the dimension required. After extrusion, the sheets are heated and embossed.

A second requirement of the matrix structure is the presence of vertical passages between layers. Several mechanical methods, drilling, punching, etc., were examined using the embossed sheets prior to stacking or burnout. However, in most cases, these techniques resulted in severe cracking. An alternative method recently investigated is laser drilling.

Presently, single embossed sheets are quickly laser drilled by a Neodymium glass pulse laser. Preliminary test results indicate that a .5 mm hole, after sintering, is produced without cracking. Laser drilling is now a practical, commercial machining technique.

Task 5. Build the Matrix Structure

Efforts have focused on the prevention of delamination, which was a problem identified earlier in the program. The objective has been to minimize or eliminate the problem by enhancing the physical bonding of tricalcium phosphate particles from neighboring layers. Simply stacking the sheets prior to binder burnout is not adequate. After several experiments, the best enhancement of the interlayer bonding was achieved by coating the surface of the embossed sheet with an oil or solvent followed by stacking, burnout, and sintering. The delamination problem has been minimized and possibly eliminated.

Task 6. Cure and Remove the Organic Binders from the Matrix

Removal of the organic binder from the matrix structure has been accomplished using a 10-day burnout cycle with a heating rate of 2°C per hour. Faster heating rates result in collapse of the structure as a consequence of melting of the binder before sufficient sublimation has occurred to produce a rigid structure. Further refinement of the binder compositions and/or burnout methods are needed to eliminate this problem.

Task 7. Sinter the Matrix Structure

After burnout, the matrix structure is heated in 1 hour to 2000°F and held at temperature for 2 hours, producing a structure with a sintered matrix density of 82 percent of theoretical. This is an outstanding improvement over the tape cast sheets which has sintered densities below 50 percent of theoretical.

Task 8. Preparation of Experimental Samples

Presently, samples are being prepared for USAIDR to specifications mutually agreed upon. These samples will be rectangular blocks designed for segmental mandibular replacement studies to be performed in animals.

Task 9. Characterization of the Matrix Structure

Work will begin after the fabrication of experimental samples has been completed.

EXPERIMENTAL ANIMAL STUDIES

This portion of the report details the various research procedures which are used in our laboratories to evaluate biodegradable materials. The procedures include histology, and radiography.

Research Protocol

In order to test the biodegradation of large tricalcium phosphate segments, a special experimental model has been devised in this laboratory. We utilize the calvarium of a mature, male, New Zealand White rabbit with a minimum weight of 8 pounds. The calvarium has been found to be an excellent test implant site for this biomaterial. Since stresses upon the calvarium are not extraordinarily high, external stabilization is not required. Consequently, confusing effects which might be due to stabilization devices are not seen. Of greater importance is the fact that this implant site provides the researcher with a large, relatively uniform area for various simultaneous studies such as periodic radiography, multiple histologic analyses, etc.

Standard aseptic surgical technique was used to expose the calvarium of the anesthetized animal. A circular, 8 mm diameter, portion of the calvarium was osteotomized bilaterally from the animal with no attempt to salvage the periosteum overlying the excised area. The tricalcium phosphate implants

were interference fit. The skin incision was closed and the animal was treated with a prophylactic antibiotic. Fourteen animals were randomly separated into four experimental groups. The experimental groups consisted of sacrifice dates, 3, 6, 9, and 12 months post implant. Since two implants were placed in each animal, four samples were available for analysis at each sacrifice interval. Two control animals were prepared. These animals had bilateral circular voids 8 mm in diameter.

The animals were radiographed at 3-month intervals until the time of necropsy. Then the excised skulls were radiographed post-necropsy. The implants were radiographed prior to surgery. A step wedge was incorporated into all radiographs to facilitate comparisons. The histologic technique consisted of embedding portions of the excised calvarium-tricalcium phosphate complex in methylmethacrylate and sectioning. Half of each excised sample was stained with basic fuchsin prior to sectioning. During the experiment, rabbits were stained at time zero and 3-month intervals with one of the following vital bone growth markers: tetracycline 60 mg/kg, DCAF 20 mg/kg and xylene orange 90 mg/kg. The other half of the above-mentioned sample was left unstained and sectioned for ultraviolet bone growth analysis utilizing these previously injected vital bone growth markers.

Radiographic Examination of Tricalcium Phosphate Biodegradability

Radiographs of the rabbits were taken at time zero, 3-month intervals and of the excised skull after necropsy to monitor the biodegradation of the tricalcium phosphate implant. These high resolution radiographs were obtained using fine-grained industrial x-ray film and a Picker Industrial X-Ray Unit.

Representative of the results are the radiographs of rabbit D-81. Figure 1 shows in situ tricalcium phosphate implants 21 days post implant. Note that the implants are readily apparent in the animals' calvarium. In this "live" x-ray detail of the directed porosity of the implant is not distinct. The radiodensity of both implants appears equivalent.



$\approx 2.5X$

FIGURE 1. RADIOGRAPH OF RABBIT D-81, 21 DAYS POST-IMPLANT

The implants are readily apparent in the animal's calvarium, shown as circular images. In this "live" X-ray, the directed porosity of the implants is not readily apparent.

Note that all radiographs in this research report were exposed with a step wedge included. The step wedge was used as a control to correct for any exposure differences. Consequently, all photographs of radiographs in this report are corrected, relative to a control density.

Figure 2 is a radiograph of the same animal (D-81) 3 months post implant. The overall radiodensity of the implants is lower, suggesting some bioresorption within the samples. The right implant is somewhat obscured by the angle of this radiograph.

By 6 months, there is a dramatic alteration in the appearance of the samples. Figure 3 illustrates the 6 month radiograph of rabbit D-81. The samples are difficult to locate in the radiograph. This suggests that the radiodensity of the samples is approaching that of the surrounding bone and further suggests additional bioresorption.

Figure 4 is the 9 month radiograph of rabbit D-81. Only under close scrutiny can remnants of the samples be found. Again, the radiograph suggests continuing resorption of the samples.

Another example of radiodensity alteration with time can be seen in a 12 month experimental animal. Figure 5 (Rabbit F) shows an x-ray taken at "zero time". The left implant is clearly visible, but unfortunately the right implant is not clear. At 12 months (Figure 6), there is a definite decrease in density seen in the left implant. The right hand implant is not visible. Another example of 12 month radiodensity change can be seen in Rabbit I. At three months (Figure 7) both implants are clearly visible. At 12 months, (Figure 8) a definite alteration in radiodensity is seen in both samples. However, there appears to be a radiolucent area posterior to the right hand implant. Also there appears to have been more resorption in the right implant than the left. It should be noted that the right implant was thinner than the left at the time of implant. It is further apparent that there is some inconsistency between animals in the degree of bioresorption which has taken place. Subjectively, it appears that resorption is slowing down at about month 9. For example, in Figure 9, (Rabbit I) at 9 months it is difficult to distinguish between this 9 month radiographs (left hand implant) and the same implant at 12 months (Figure 8). This observation is opposite to the expected result. One would anticipate an increase in resorption rate with time, due to an increase in the surface area to volume ratios.

A better view of bioresorption can be obtained from excised skulls. Since sequential radiographs of the same animal cannot be obtained, serial necropsies at radiographs 3 month intervals are presented here. Each implant



≈ 2.5X

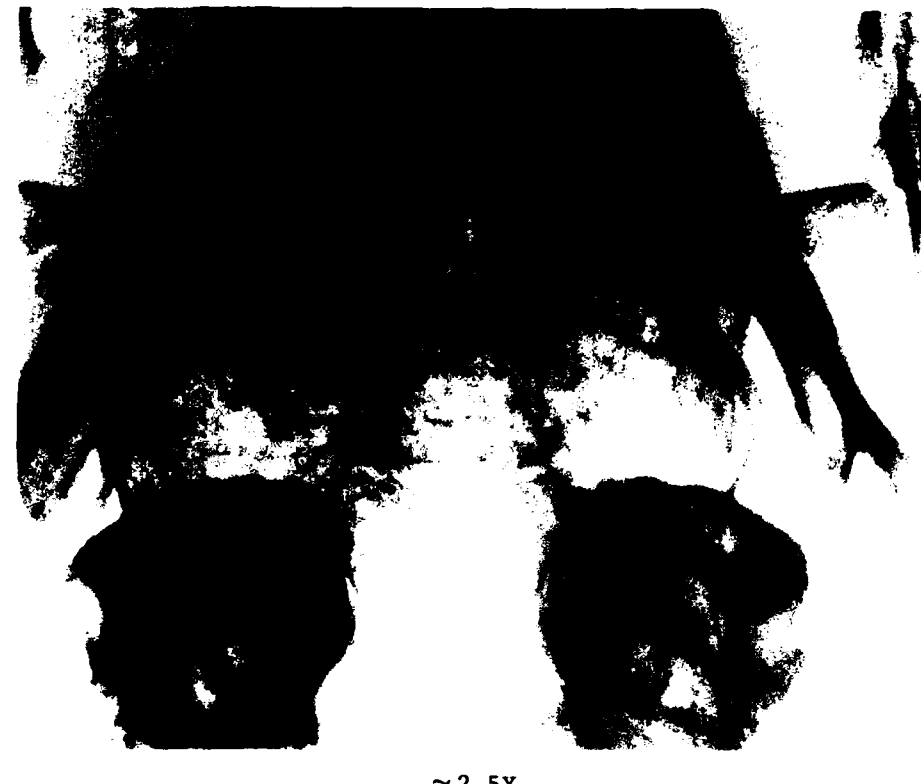
FIGURE 2. RADIOGRAPH OF RABBIT D-81, 3 MONTHS POST-IMPLANT

This radiograph shows a decrease in overall radiodensity when compared to the previous figure. This suggests some biore sorptive activity of the implanted samples.



FIGURE 3. RADIOGRAPH OF RABBIT D-81, 6 MONTHS POST-IMPLANT

This figure demonstrates a dramatic decrease in the radio-density of these samples when compared to the previous two figures. This suggests progressive bioresorption. The density of the biomaterial now approximates that of the surrounding bone.



≈ 2.5X

FIGURE 4. RADIOGRAPH OF RABBIT D-81, 9 MONTHS POST-IMPLANT

In this figure, bioreresorption is apparently extensive, remnants of the samples can be found only under close scrutiny. This is the same animal illustrated in the preceding three figures.



≈ 2.5X

FIGURE 5. RADIOGRAPH OF RABBIT F-81,
IMMEDIATELY POST-IMPLANT

This figure presents another example of directed porosity implants shortly after surgery.



≈ 2.5X

FIGURE 6. RADIOGRAPH OF RABBIT F-81, 12 MONTHS POST-IMPLANT

When compared to Figure 5, the radiodensity has decreased dramatically as the previous example. In this figure, there appears to be preferential resorption in the right implant and along the directed pores. The pore diameters appear to be increasing.



≈2.5X

FIGURE 7. RADIOGRAPH OF RABBIT I-81, 3 MONTHS POST-IMPLANT
At this time, both samples are clearly visible.



≈2.5X

FIGURE 8. RADIOGRAPH OF RABBIT I-81, 12 MONTHS POST-IMPLANT

When compared to Figure 7, there has been a definite decrease in the apparent radiodensity of the tricalcium phosphate implants. Further there appears to be a radio-lucent area posterior to the right hand implant.



≈ 2.5X

FIGURE 9. RADIOGRAPH OF RABBIT I-81, 9 MONTHS POST-IMPLANT

In this particular animal it is difficult to distinguish between this radiograph and that taken 3 months later. Subjectively resorption appears to have slowed. This is not consistently observed in all experiments.

is presented directly above a preimplant radiography of the identical specimen. This method provides an evaluation of resorption rate for the time period noted.

Figure 10 illustrates a 3-month necropsy radiograph of an excised skull (Rabbit G-81). The samples can be clearly observed in this radiograph because interfering bone and tissue structures have been removed. The same implants are illustrated below as they appeared when radiographed prior to surgery. Upon comparison, some resorption of the implants and ingrowth can be noted by widening of the directed pores and the appearance of granular material (presumably bone) within the pores. Granular-appearing material is especially noticeable in the left implant.

Figure 11 illustrates a 6-month necropsy radiograph (Rabbit E-81). Again, a radiograph of the same samples prior to implant is included below for comparative purposes. When compared to the pre-surgery radiograph, considerable resorption of the sample and ingrowth of bone is suggested. The degree of resorption can be readily noted in the holes normal to the film plane. Their diameter has markedly increased in the six-month experimental period.

Figure 12 represents a 9-month necropsy radiograph (Rabbit D-81). Note that very significant bioresorption and bone ingrowth appears to have taken place. The change in these samples is especially dramatic when they are compared to either their control radiographs or those examples of 3- and 6-month animals. It is significant to note that there has been no loss of bone integrity. Loss of bone integrity or bone resorption when it occurs is usually noted by the radiographic appearance of large radiolucent areas.

Figure 13 represents a 12-month necropsy radiograph (Rabbit F-81). Here an impressive degree of bioresorption can be noted in both samples. The result is much more obvious in the right hand sample. This sample was thinner than the left sample at the time of implant. However, even the thicker left hand sample shows an impressive degree of internal resorption.

Figure 14 is a 12-month necropsy radiograph of a control animal (Rabbit N-81) in which holes were cut but no samples placed. This control animal clearly illustrates that a defect of this size and type will not naturally heal.



A



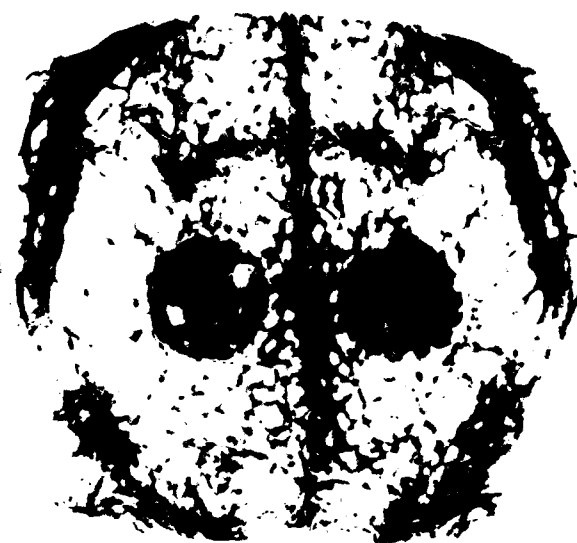
B

 $\approx 2.5X$

FIGURE 10. THREE-MONTH POST-NECROPSY RADIOGRAPH OF EXCISED CALVARIUM FROM RABBIT G-81

In Panel A, the large directed porosity of the samples are clearly visible because the interfering bone and tissue structures have been removed. In Panel B, a radiograph of the same implants prior to surgery is presented for comparison. The identical implants are located directly above. However, the implants were rotated at surgery.

The comparison of the two radiographs shows resorption as evidenced by widening and decreased radiodensity especially along the pores, and apparent ingrowth as evidenced by granular material within the pores.



A



B

 $\approx 2.5X$

FIGURE 11. SIX-MONTH POST-NECROPSY RADIOPHGRAPH OF EXCISED CALVARIUM FROM RABBIT E-81

In Panel A, the samples are shown in the excised calvarium at six months post-implant.

In Panel B, the same samples are shown prior to surgery. As in the previous example (Figure 10), bioresorption and bone ingrowth appears to be under way. Resorption appears more advanced than at 3 months.



A

 $\sim 2.5X$

FIGURE 12. NINE-MONTH POST-NECROPSY RADIOGRAPH OF EXCISED CALVARIUM FROM RABBIT D-81

In Panel A, the samples are shown as they appear nine-months post-implant. In Panel B, the same implants are shown as they appeared prior to surgery.

In this figure, the apparent bioresorption and bone ingrowth is dramatic when compared to control, or to the 3- and 6-month samples (Figures 10 and 11). It is significant to note that there has been no bone loss.



A



B

 $\approx 2.5X$

FIGURE 13. TWELVE-MONTH POST-NECROPSY RADIOPHOTOGRAPH OF EXCISED CALVARIUM FROM RABBIT F-81

In Panel A, the samples are shown as they appear 12 months post implant. In Panel B, the same implants are shown as they appeared prior to surgery. Extensive resorption is seen in both samples. However, resorption is much more complete on the right, where a somewhat thinner implant was used.



≈2.5X

FIGURE 14. TWELVE-MONTH POST-NECROPSY RADIOPHOTOGRAPH OF EXCISED CALVARIUM FROM RABBIT N-81

This radiograph is from a control animal. The results indicate that a void of this size in the rabbit calvarium will not heal naturally.

Histologic Evaluations

To evaluate the rate of ingrowth of biologic material (bone and connective tissue) into the tricalcium phosphate and the subsequent biodegradation of tricalcium phosphate, ground sections of the excised skulls were prepared. A methylmethacrylate embedding technique was used. Due to the nature of tricalcium phosphate, ground sections cannot be prepared without embedding in a rigid fixation medium such as methylmethacrylate. Sections have been prepared both pre-stained with basic fuchsin and also unstained.

Figure 15 is a photomicrograph of a specimen implanted for 3 months (Rabbit G-81-3L). Both transverse and longitudinal pores can be seen. Rather extensive bone formation is seen in the lower longitudinal pore. However, mostly dense connective tissue fills the upper longitudinal pore. Between the two longitudinal pores are the scalloped shapes produced by transverse pores which are extending at right angles to the plane of the figure. These pores are filled with bone, some connective tissue and diploë-like spaces, which apparently contain marrow.

Figure 16 is a photomicrograph from another three month animal (Rabbit B-81-5T). This figure presents a somewhat different appearance than the previous figure. In a longitudinal pore (shown at the bottom of the figure) bone appears to be closely adapted to the tricalcium phosphate wall of the pore, whereas the central portion of the pore appears to contain voids similar to those normally seen in the diploë layer of calvarium bone. The diploë is generally trabecular like bone with marrow filling most of the void spaces. The old bone is at the left and bone ingrowth appears to be proceeding into the large pores. Bone within the biomaterial appears similar in morphology to the old bone.

Figure 17 is a higher magnification of the same area (Rabbit B-81-5T). Note the close adaptation of bone to the tricalcium phosphate. Osteoblast-like cells appear to be lined up at the bone-biomaterial interface.

Figure 18 is a photomicrograph from a 6-month experiment (Rabbit A-81-5L). All available pore spaces appear to be packed with bone or diploë-like spaces filled with marrow. Generally, bone occupies all the available biomaterial interface space. Figure 19 is a photomicrograph of the



≈ 37X

FIGURE 15. PHOTOMICROGRAPH OF TRICALCIUM PHOSPHATE SPECIMEN WITH DIRECTED POROSITY, THREE MONTHS POST-IMPLANT (RABBIT G-81-3L)

This figure shows one longitudinal pore in the lower portion of the figure with bone ingrowth. The upper longitudinal pore is filled with connective tissue. The transverse pores, seen in the middle of the figure appear as scalloped shapes. These pores are at right angles to the pore layers above and below. These pores contain bone, some connective tissue and marrow-filled spaces similar to those normally seen in the diploë of rabbit calvaria.

Note: Included in the rabbit identification, is the slide number from which the particular photomicrograph was obtained. For example, in this figure, -3L identifies the slide number.



≈ 37X

FIGURE 16. PHOTOMICROGRAPH OF TRICALCIUM PHOSPHATE SPECIMEN WITH DIRECTED POROSITY, THREE MONTHS POST-IMPLANT (RABBIT B-81-5T)

This implant exhibits bone ingrowth preferentially at the bone biomaterial interface. The longitudinal pore at the bottom of the figure shows bone closely adapted to the tricalcium phosphate. The center of the pore contains marrow space. The bone appears to have grown from the old bone, at the left, unimpeded by the presence of the biomaterial.



≈ 90X

FIGURE 17. PHOTOMICROGRAPH OF BONE INGROWTH INTO LONGITUDINAL
PORE AT HIGH MAGNIFICATION, THREE MONTHS POST-IMPLANT
(RABBIT B-81-5T)

This view shows the close adaptation between bone and tricalcium phosphate. There does not appear to be a continuous connective tissue layer at this interface. Osteoblast-like cells appear lined up at the bone-biomaterial interface.



≈37X

FIGURE 18. PHOTOMICROGRAPH OF BONE INGROWTH INTO TRICALCIUM PHOSPHATE, SIX MONTHS POST-IMPLANT (RABBIT A-81-5L)

At six months, all available spaces within the implant appear densely packed with bone and marrow spaces. As seen previously bone is predominantly seen at the biomaterial interface.



≈ 37X

FIGURE 19. PHOTOMICROGRAPH OF BONE INGROWTH INTO TRICALCIUM PHOSPHATE, SIX MONTHS POST-IMPLANT (RABBIT A-81-5T)

This figure demonstrates extensive bioresorption of the tricalcium phosphate. The walls of biomaterial between the pores have been reduced to spicules. As in previous figures all available space is packed with bone and/or marrow space. The consistency of the bone approximates that of normal calvarium.

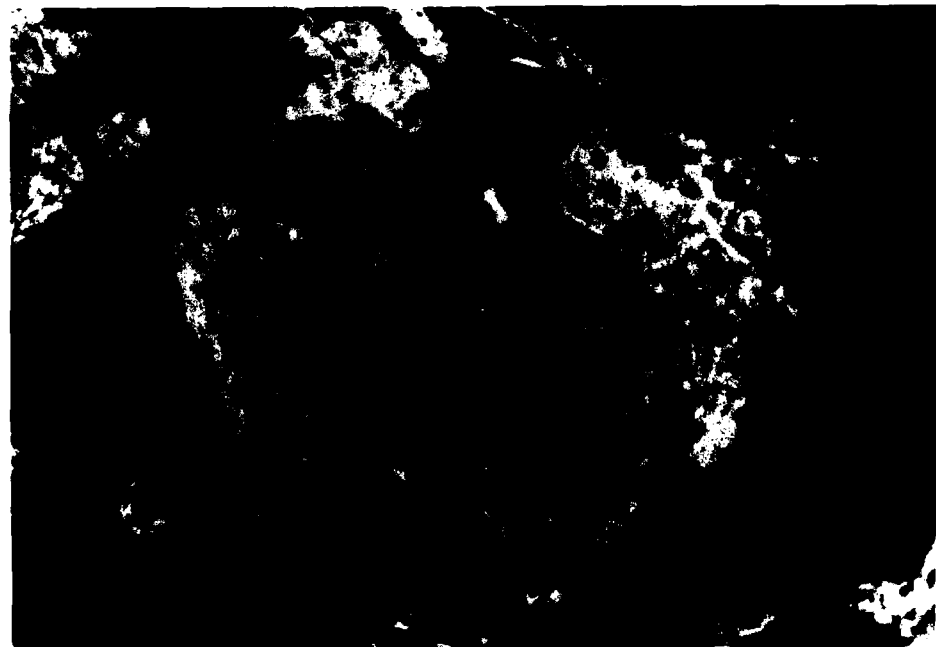
contralateral tricalcium phosphate implant (Rabbit A-81-5T). Again, bone and diploë marrow spaces are seen filling the available biomaterial pore space. However, in this sample it appears that considerably more bioresorption has taken place as evidenced by the thin spicules of tricalcium phosphate that remain.

Figure 20 is a higher magnification photomicrograph from a 6-month implant specimen (Rabbit E-81-4T). In this case, a transverse pore is shown. As noted previously, bone appears to adapt closely to the biomaterial whereas the central portion of the pore is filled with a non-osseous, diploë-like space filled with marrow.

Figure 21 is a photomicrograph from a 9 month specimen (Rabbit C-81-LFC). This particular section is unusual in that the degree of bioresorption is extreme, as compared to 12 month samples. This example indicates that variability was observed, in terms of interspecimen resorption rate. This particular unstained section does not show good bone detail. However, the pattern is consistent with the previously presented photomicrograph: bone close adapted to the tricalcium phosphate with open diploë appearing spaces. Blood formed elements are not visible in this preparation.

Figure 22 illustrates a 12 month photomicrograph (Rabbit F-81-L2). The resorption process is not as obvious as the previous 9 month example. However, the internal structure of the implant is well on its way to being replaced with bone. It is significant to note, that mechanical integrity of the implant or surrounding bone was not lost in this animal any of the experimental animals.

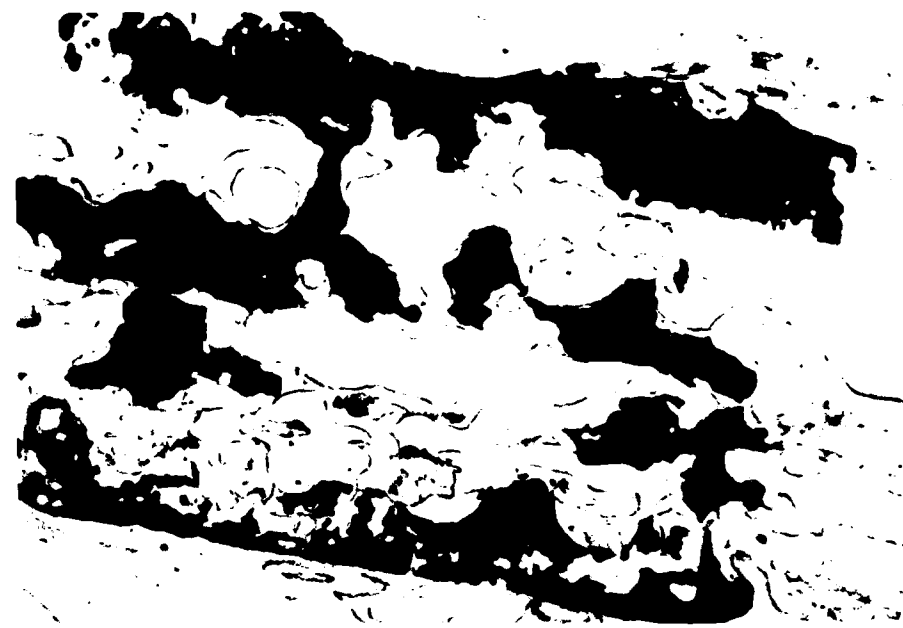
Figure 23 is a high magnification photomicrograph of a 12 month animal (Rabbit F-81-L2). Again the consistent pattern of close adaptation of bone to the tricalcium phosphate is present. The bone structure again has typical diploë-like spaces. This area of the implant appears to contain a higher percentage of bone than implant, thus indicating significant resorption. The two previous photomicrographs are from the left hand sample from rabbit F, as shown in the radiographs of that animal. Figure 24 is a photomicrograph of a 12-month control animal which was not implanted (Rabbit N-81-L1). Note that the void area is bridged by connective tissue, and bone formation has occurred only at the periphery of void. This figure illustrates that the size of void used will not naturally be repaired by bone ingrowth.



≈90X

FIGURE 20. PHOTOMICROGRAPH OF TRICALCIMUM PHOSPHATE SIX MONTHS POST-IMPLANT (RABBIT E-81-4T)

This figure at high magnification shows the close adaptation of bone to the biomaterial. The periphery of the pore contains dense bone, whereas the central pore area contains marrow space.



≈ 37X

FIGURE 21. PHOTOMICROGRAPH OF BONE INGROWTH INTO TRICALCIMUM PHOSPHATE, NINE MONTHS POST-IMPLANT (RABBIT C-81-LFC)

This unstained specimen demonstrates extensive bioresorption of the tricalcium phosphate.

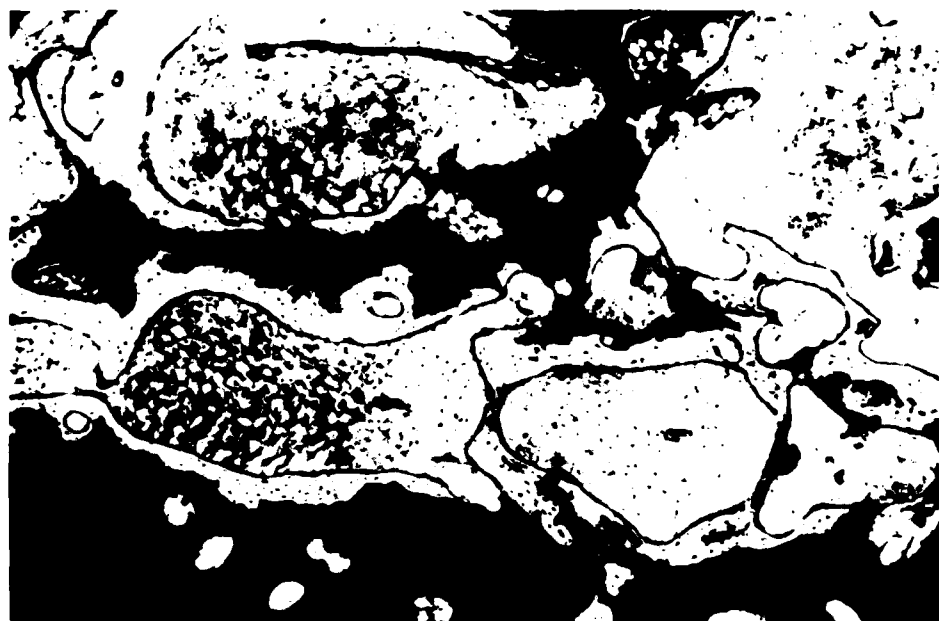
This particular 9 month implant underwent more resorption and subsequent bone replacement than most comparable samples. It is significant that mechanical integrity was not lost, even with the extreme example of resorption.



≈37X

FIGURE 22. PHOTOMICROGRAPH OF BONE INGROWTH INTO TRICALCIMUM PHOSPHATE, TWELVE MONTHS POST-IMPLANT (RABBIT F-81-L2)

This figure demonstrates less extensive bioresorption of tricalcium phosphate than seen in the previous 9 month example (Figure 21). Some 12 month specimens exhibit more extensive resorption for example, Figure 13.



≈90X

FIGURE 23. PHOTOMICROGRAPH OF BONE INGROWTH INTO TRICALCIUM PHOSPHATE, TWELVE MONTHS POST-IMPLANT
(RABBIT F-81-L2)

This figure demonstrates extensive bioresorption of the tricalcium phosphate histologically consistent having an appearance consistent with other specimens observed at high magnification.



≈37X

FIGURE 24. PHOTOMICROGRAPH OF BONE INGROWTH INTO A CONTROL ANIMAL TWELVE MONTHS POST-SURGERY (RABBIT N-81-5L)

This figure demonstrates that bone ingrowth will not naturally occur into the void used in this experiment.

CONCLUSIONS AND DISCUSSION

This study indicates that the use of longitudinally organized unidirectional implant pores is a viable method to prevent the deleterious loss of implant and bone integrity. Such loss of integrity was seen in previous experiments when omnidirectional materials were studied.

Integrity has continually plagued the use of omnidirectional structural bioresorbable bone scaffold materials. The omnidirectional design has two major drawbacks. First, the initial strength of the material is severely limited. Second, and more importantly, as bone grows in and the material simultaneously biodegrades, mechanical integrity of the biomaterial-bone complex is usually lost. The result is a bone loss and filling of the area with connective tissue in response to loss of stability. With the unidirectional material presented in this report, the use of relatively large channels for bone to grow through, coupled with a stronger wall material, appears to provide adequate mechanical integrity during the resorption process to prevent bone loss.

This report provides animal data up to 12 months post implant on material termed "second generation". This material had relatively large and directional pores of approximately 450 microns. The pores were running at 90° alternating direction every layer. This material suffered from low mechanical strength at the interfaces of the sheet laminates used to construct the composite. It also had less than the desired distribution of cross connections. Despite these problems the material had vastly improved bulk strength properties as compared to omnidirectional or first generation unidirectional materials. The improved strength opens up numerous additional possibilities for the potential application of the material. An obvious advantage is that less external fixation will be required when this material is utilized. The material will also be able to accommodate more loading during the bone ingrowth, remodeling and implant resorption.

The most important finding of this study is the extensive biodegeneration of the tricalcium phosphate scaffold material without loss of mechanical integrity of the ingrowing and remodeling bone. At 12 months, there is

still residual material. Consequently, the ultimate fate of this material has yet to be determined.

Another difficulty noted was the lack of consistency in resorption rate, especially between 9 and 12 months. Some 9 month samples appeared to have proceeded as far as similar samples at 12 months. The most probable explanation for this difference is biological variability. It should also be noted that in an attempt to match the rabbit skull thickness, different thicknesses of implant were used. Since the material is of "layered" construction removing a small amount of material will potentially uncover a whole layer of pores. In such a fashion the surface area to volume ratio may be dramatically altered. This is one difficulty with the present calvarium model when a relatively thick material is placed in a thin skull. However, the model is realistic in the sense that the biomaterial sample is not unduly stressed by a large mass of surrounding bone.

To minimize interpretation difficulties the samples were radiographed before surgery at their actual implant thickness. Thus, by comparison to the preimplant radiograph a true evaluation of resorption of any particular sample can be obtained.

The parallel material development aspect of this project has produced further improvements in the material. The newest material is termed "third generation". This material appears the same in overall configuration, however, it is dramatically improved in two aspects. First, interlayer bonding problem has been minimized or virtually eliminated. Second, the strength of the material has been further enhanced.

The third generation material still has less than the desired number of cross connections between pores and layers. A second difficulty is a change in source of raw material supply. Our previous supplier of calcium carbonate has ceased production. The same material supplied by alternate manufacturers does not produce a satisfactory product. Presently, technique modifications are being implemented to eliminate this difficulty.

In summary, the outcome for successful healing of the bone void via scaffold ingrowth and resorption appears favorable. The biomaterial being used appears to be adequate in overall design. The basic methodology of material construction appears to be practical for volume production. This

method will allow for the construction of numerous variations based upon the same basic design concept. One can envision materials designed for various bone replacement uses within the body. Pore direction can be manufactured as desired by the user. Even further improvements in mechanical properties of the material are possible.

RECOMMENDATIONS

The concept of directed porosity has now been shown viable in several different experimental series. An improved "third generation" material with greatly improved physical properties will shortly be available. In vivo evaluations should be performed on the third generation material at Battelle-Columbus in the calvarium model and dog mandible experiments at USAIDR.

REFERENCES

- (1) Bhaskar, S. N., Cutright, D. E., Knapp, M. J., Beasley, J. D., and Perez, B., "Tissue Reactions to Intrabone Ceramic Implants", Oral Surg., Oral Med., Oral Path., 31:282-289 (February, 1971).
- (2) Bhaskar, S. N., Brady, J. M., Getter, L., Grower, M. F., and Driskell, T. D., "Biodegradable Ceramic Implants in Bone (Electron and Light Microscopic Analysis)": Oral Surg., Oral Med., Oral Path., 32:336-346 (August, 1971).
- (3) Getter, L., Bhaskar, S. N., Cutright, D. E., Bienvenido, P., Brady, J. M., Driskell, T. D., O'Hara, M. J., "Three Biodegradable Calcium Phosphate Slurry Implants in Bone", J. of Oral Surgery, 30:263-268 (April, 1972).
- (4) Driskell, T. D., O'Hara, M. J., and Greene, G. W., Jr., D.D.S., "Management of Hard Tissue Avulsive Wounds and Management of Orofacial Fractures", Report No. 1, Contract No. DADA17-69-C-9118, February 1, 1971.
- (5) Driskell, T. D., O'Hara, M. J., and Grode, G. A., "Management of Hard Tissue Avulsive Wounds and Management of Orofacial Fractures", Report No. 2, Contract No. DADA17-69-C-9118, October, 1971.
- (6) Driskell, T. D., O'Hara, M. J., Niesz, D. E., and Grode, G. A., "Management of Hard Tissue Avulsive Wounds and Management of Orofacial Fractures", Report No. 3, Contract No. DADA17-69-C-9118, October, 1972.
- (7) McCoy, L. G., Hassler, C. R., Wright, T. R., Niesz, D. E., "Management of Hard Tissue Avulsive Wounds and Management of Orofacial Fractures", Report No. 4, Contract No. DADA17-69-C-9118, July, 1974.
- (8) McCoy, L. G., Hassler, C. R., and Niesz, D. E., "Management of Hard Tissue Avulsive Wounds and Management of Orofacial Fractures", Report No. 5, Contract No. DADA17-69-C-9118, June, 1976.
- (9) McCoy, L. G. and Hassler, C. R., "Management of Hard Tissue Avulsive Wounds and Management of Orofacial Fractures", Report No. 6, Contract No. DADA17-69-C-9118 (August 15, 1980).
- (10) Hassler, C. R. and McCoy, L. G., "Management of Hard Tissue Avulsive Wounds and Management of Orofacial Fractures", Report No. 7, Contract No. DADA17-69-C-9118 (May 31, 1981).
- (11) Tortorelli, A. F. and Posey, W. R., Bone Ingrowth and Replacement of "Ceramic in Mandibular Continuity Defects", Jour. Dental Res. 60A:1168 (1980).
- (12) Hassler, C. R. and McCoy, L. G., "Management of Hard Tissue Avulsive Wounds and Management of Orofacial Fractures", Report No. 8, Contract DADA17-69-C-9118 (May 31, 1982).

4 copies

Commander
U.S. Army Medical Research
and Development Command
ATTN: (SGRD-RMS)
Frederick, Maryland 21701-5012

12 copies

Administrator Defense Technical
Information Center
ATTN: DTIC-DOA
Cameron Station
Alexandria, Virginia 22304-6145

1 copy

Commandant
Academy of Health Sciences, US Army
ATTN: AHS-CDM
Fort Sam Houston, Texas 78234-6100

1 copy

Dean
School of Medicine
Uniformed Services University
of the Health Sciences
4301 Jones Bridge Road
Bethesda, Maryland 20814-4799

END

FILMED

10-85

DTIC